Second-order synchrosqueezing transform or invertible reassignment? Towards ideal time-frequency representations

Thomas Oberlin, Sylvain Meignen, Valérie Perrier

Second-order synchrosqueezing transform or invertible reassignment? Towards ideal time-frequency representations

Thomas Oberlin*, Sylvain Meignen, and Valérie Perrier

Thomas Oberlin
Inria Rennes
Campus de Beaulieu
35042 Rennes
France
tel. +33 (0)2 99 84 72 62
thomas.oberlin@inria.fr

Sylvain Meignen
Jean Kuntzmann Laboratory
Grenoble-Alpes University
51 rue des Mathématiques
38041 Grenoble cedex 09
France
tel. +33 (0)4 76 51 43 95
sylvain.meignen@imag.fr

Valérie Perrier
Jean Kuntzmann Laboratory
Grenoble-Alpes University
51 rue des Mathématiques
38041 Grenoble cedex 09
France
tel. +33 (0)4 76 51 45 51
valerie.perrier@imag.fr

Abstract

This paper considers the analysis of multicomponent signals, defined as superpositions of real or complex modulated waves. It introduces two new post-transformations for the short-time Fourier transform, that achieve a compact time-frequency representation while allowing for the separation and the reconstruction of the modes. These two new transformations thus provide the benefits of both the synchrosqueezing transform (which allows for reconstruction) and the reassignment method (which achieves a compact time-frequency representation). Numerical experiments on real and synthetic signals demonstrate the efficiency of these new transformations, and illustrate their differences.

Index Terms

time-frequency, reassignment, synchrosqueezing, AM/FM, multicomponent signals.

EDICS Category: DSP-TFSR, DSP-TRSF

S. Meignen and V. Perrier are with the Jean Kuntzmann Laboratory, University of Grenoble-Alpes and CNRS, Grenoble, France.

Thomas Oberlin (corresponding author) is with teams Visages and Panama, INRIA, Rennes, France.

The authors acknowledge the support of the French Agence Nationale de la Recherche (ANR) under reference ANR-13-BS03-0002-01 (ASTRES).

Second-order synchrosqueezing transform or invertible reassignment? Towards ideal time-frequency representations

I. Introduction

Most real signals can be accurately modeled as superpositions of locally bandlimited, amplitude and frequency-modulated (AM-FM) waves. Containing several modes they are often called multicomponent signals (MCS). Many approaches have been built to decompose these signals into their constituent modes either in time-frequency (TF) domain, like the synchrosqueezing transform [1], or in time domain, as for instance the empirical mode decomposition (EMD) [2], [3]. Yet, very few results on the accuracy of the mode retrieval are available. In this regard, a new approximation result on the retrieval of weakly modulated modes of an MCS has been shown using the synchrosqueezing transform (SST) [4]. To obtain such a result, very strong assumptions were made on the modes making up the signal among which the most limitating one is the weak modulation hypothesis on the modes.

Indeed, most MCS contain strongly frequency modulated modes, as for instance chirps involved in radar [5], speech processing [6], or graviational waves [7]. Although many TF transforms such as quadratic distributions [8], [9] or the reassignment method (RM) [10], [11] manage to accurately represent this kind of signals, they do not allow for mode separation and reconstruction. Recently, some work has been done on how to deal with high FM with SST. For instance, in [12], authors use a two-steps algorithm, which first computes SST, estimates the FM, and finally recomputes SST on the demodulated mode. In the same spirit, authors in [13] use an iterative procedure, where at each iteration a SST is computed with a finer resolution. A different and earlier attempt [14] consisted in building an invertible extension of RM. Unfortunately, the proposed reconstruction was only an approximation, valid for Gaussian windows with a small temporal width.

The aim of this paper is to extend SST to MCS containing strongly frequency modulated modes by generalizing the SST in two different ways. The first attempt is inspired by RM, which is known to optimally sharpen the TF representation of a linear chirp. However, in the original RM the sharpened representation obtained from the spectrogram did not allow for mode retrieval. We will see that by fully exploiting the information contained in the so-called *reassignment vector*, one can derive a new

generation of SST that provides a sharpened TF representation as good as the one given by RM, while enabling exact retrieval of linear chirps. Our second approach relies on a second-order local estimate of the instantaneous frequency, which is used to improve modes localization and reconstruction using SST.

The outline of the paper is as follows: in section II, we recall important notations that are subsequently used in the paper and we introduce the concept of weakly modulated modes. We then define SST and RM in section III, putting the emphasis on the differences in terms of reconstruction and representation. Then, section IV is devoted to the presentation of the new extensions of SST. Section V finally delivers numerical results on both synthetic and real data, comparing the proposed methods with standard SST and RM.

II. Time-frequency analysis of multicomponent signals

A. Short-Time Fourier Transform

Definition II.1. *The Fourier transform of a function $f \in L^1(\mathbb{R})$ is defined by*

$$\hat{f}(\eta) = \int_{\mathbb{R}} f(t) e^{-2i\pi\eta t}\, dt. \tag{1}$$

For a given η, $\hat{f}(\eta)$ represents the part of f that oscillates at frequency η on the whole time domain. The need for time-localized frequency descriptors leads to the following definition:

Definition II.2. *Let $g \in L^2(\mathbb{R})$ a real-valued and even function, with unit norm. The short-time Fourier transform (STFT) of $f \in L^2(\mathbb{R})$, with respect to the window g, is defined by*

$$V_f^g(\eta, t) = \langle f, g_{\eta,t} \rangle = \int_{\mathbb{R}} f(\tau) g(\tau - t) e^{-2i\pi\eta(\tau - t)}\, d\tau. \tag{2}$$

The representation of the positive quantity $|V_f^g(\eta, t)|^2$ in the TF plane is called the spectrogram *of f. Without ambiguity, V_f^g will be denoted by V_f.*

Remark: The usual definition of STFT differs from equation (2) by a factor $e^{2i\pi\eta t}$ and considers the conjugate of g. However, to be consistent with the continuous wavelet transform formulation that follows we stick to equation (2). Also, as we assume g to be real-valued, we do not need the conjugate g^* in (2).

It is well known from the properties of the Fourier transform that a well-localized TF representation requires a window g well localized both in time and frequency. We shall then mention that STFT is

invertible on $L^2(\mathbb{R})$ using either of the following formulae:

$$f(\tau) = \iint_{\mathbb{R}^2} V_f(\eta, t) g(\tau - t) e^{2i\pi\eta(\tau - t)}\, dt d\eta \tag{3}$$

$$f(\tau) = \frac{1}{g(0)} \int_{\mathbb{R}} V_f(\eta, t) d\eta. \tag{4}$$

Note that equation (4) is valid only if g is non-zero and continuous at 0. If the signal is analytic (i.e. $\eta \leq 0 \Rightarrow \hat{f}(\eta) = 0$) then the integral domain for η is $\mathbb{R}_+$.

B. Continuous Wavelet Transform

STFT can be interpreted as the scalar product of f onto the translated and dilated versions of window g, each basis functions having the same TF resolution. On the contrary, the continuous wavelet transform (CWT) is associated with the decomposition of a signal on a family of functions with varying TF resolution [15], [16]. Let us recall briefly its definition:

Definition II.3. *An admissible wavelet is a function $\psi \in L^2(\mathbb{R})$ satisfying the condition*

$$0 < C_\psi = \int_0^\infty |\hat{\psi}(\eta)|^2 \frac{d\eta}{\eta} < \infty. \tag{5}$$

Definition II.4. *Let $f \in L^2(\mathbb{R})$ and ψ be an admissible wavelet, the continuous wavelet transform (CWT) of f is defined for each $(a, t) \in \mathbb{R}_+^* \times \mathbb{R}$ by:*

$$W_f(a, t) = \langle f, \psi_{a,t} \rangle = \frac{1}{a} \int_{\mathbb{R}} f(\tau) \psi \left(\frac{\tau - t}{a} \right)^* d\tau. \tag{6}$$

The representation $|W_f(a, t)|^2$ in the time-scale plane is called the scalogram *of f.*

It is well known [15] that when ψ is real, the transform is invertible:

$$f(\tau) = \frac{1}{C_\psi} \iint_{\mathbb{R}_+^* \times \mathbb{R}} W_f(a, t) \frac{1}{a} \psi \left(\frac{\tau - t}{a} \right) \frac{dadt}{a}. \tag{7}$$

As in the STFT case, another reconstruction formula exists, which consists in the following integral:

$$f(\tau) = \frac{1}{C'_\psi} \int_0^\infty W_f(a, \tau) \frac{da}{a}, \tag{8}$$

where the constant $C'_\psi = \int_{\mathbb{R}} \frac{\overline{\hat{\psi}(\eta)}}{\eta} d\eta$ is supposed to be finite. Similarly to the STFT case, a good TF localization imposes some constraints on the wavelet ψ.

To properly deal with real signals, one needs to associate with these signals only positive frequencies, that is to consider the analytic signal $f_a = (\mathcal{I} + i\mathcal{H})f$, where $\mathcal{H}f$ is the Hilbert transform of f. Then,

when one uses *analytic* wavelets (i.e. satisfying $\eta \leq 0 \Rightarrow \hat{\psi}(\eta) = 0$), f can be reconstructed from the CWT of its analytic signal f_a since:

Proposition II.1. *Let $f \in L^2(\mathbb{R})$ be a real-valued signal, and ψ an admissible analytic wavelet (satisfying $\nu \leq 0 \Rightarrow \hat{\psi}(\nu) = 0$). Denote by $f_a = (\mathcal{I} + i\mathcal{H})f$ the analytic signal associated to f, then $W_f = \frac{1}{2}W_{f_a}$. In particular, the following synthesis stands in $L^2(\mathbb{R})$:*

$$f(\tau) = \mathcal{R}e\left\{\frac{2}{C_\psi}\int_0^\infty \int_{\mathbb{R}} W_f(a,t)\frac{1}{a}\psi\left(\frac{\tau - t}{a}\right)\frac{dtda}{a}\right\}, \tag{9}$$

This result shows that the use of an analytic wavelet enables to deal with real signals the same as complex ones.

C. MCS and Ridges

Definition II.5. *An AM–FM mode is an oscillating function $h(t) = A(t)e^{2i\pi\phi(t)}$, with A and ϕ' positive and slow-varying.*

$A(t)$ is called the instantaneous amplitude of h at time t, $\phi'(t)$ being its instantaneous frequency. Note that the slow-varying condition is not quantified, since as we will see later, it is model-dependent. Thanks to that condition, a first order expansion of the phase combined with a zeroth order expansion of the amplitude lead to the approximation, for τ close to a fixed time t:

$$h(\tau) \approx \tilde{h}_t(\tau) = A(t)e^{2i\pi[\phi(t)+\phi'(t)(\tau-t)]}. \tag{10}$$

STFT and CWT of mode h are then approximated by:

$$\begin{aligned} V_h(\eta,t) &\approx V_{\tilde{h}_t}(\eta,t) = h(t)\hat{g}(\eta - \phi'(t)) \\ W_h(a,t) &\approx W_{\tilde{h}_t}(a,t) = h(t)\hat{\psi}(a\phi'(t))^*. \end{aligned} \tag{11}$$

This shows that the STFT (resp. CWT) of an AM–FM mode is non-zero on a TF (resp. time-scale) strip, centered on the *ridge* corresponding to its instantaneous frequency and defined by $\eta = \phi'(t)$ for STFT and $a = \frac{\eta_\psi}{\phi'(t)}$ for CWT, $\eta_\psi = \arg\max_\eta |\hat{\psi}(\eta)|$ being the center frequency of the wavelet. Without loss of generality, we shall assume in the sequel that $\eta_\psi = 1$. The width of this strip depends on that of the support of $\hat{g}$ (resp. $\hat{\psi}$). Let us now define MCS, that are superpositions of AM-FM modes.

Definition II.6. *A MCS reads*

$$f(t) = \sum_{k=1}^{K} f_k(t) = \sum_{k=1}^{K} A_k(t) e^{2i\pi\phi_k(t)},$$

where the modes f_k satisfy $\phi'_K > \cdots > \phi'_k > \cdots > \phi'_1 > 0$.

In order to retrieve each mode from the STFT (resp. CWT) of f, we assume the modes occupy non-overlapping regions in TF (resp. TS) plane. This requires the following frequency separation condition:

Definition II.7. *If $\operatorname{supp} \hat{g} \subset [-\Delta, \Delta]$, a MCS f is separated for STFT if the instantaneous frequencies satisfy for each $k \in \{1, \cdots, K-1\}$:*

$$\phi'_{k+1} - \phi'_k > 2\Delta.$$

If $\operatorname{supp} \hat{\psi} \subset [1-\Delta, 1+\Delta]$, a MCS f is separated for the CWT if for each $k \in \{1, \cdots, K-1\}$:

$$\frac{\phi'_{k+1} - \phi'_k}{\phi'_{k+1} + \phi'_k} > \Delta.$$

Note that this separation condition is of a linear (resp. logarithmic) type for STFT (resp. CWT). Note also that for non-compactly supported windows (e.g. the Gaussian window) or wavelets, these conditions can be adapted by defining Δ as the "essential support".

III. Synchrosqueezing and Reassignment in a Nutshell

The so-called reassignment method (RM) [11] is a general way to sharpen a TF representation towards its *ideal TF representation* which corresponds for MCS given by definition II.6 to:

$$\mathrm{TI}_f(\eta, t) = \sum_{k=1}^{K} A_k(t)^s \delta(\eta - \phi'_k(t)), \tag{12}$$

s being equal to 1 or 2 depending on whether a linear or a quadratic representation is used (e.g. $s = 2$ for the spectrogram and $s = 1$ for STFT).

A. Reassignment of the Spectrogram

RM presented here in the spectrogram context consists of the computation of so-called *reassignment operators*:

$$\begin{aligned}\hat{\omega}_f(\eta,t) &= \frac{1}{2\pi}\partial_t \arg V_f(\eta,t) = \eta + \mathcal{I}m\left\{\frac{1}{2\pi}\frac{V_f^{g'}(\eta,t)}{V_f^g(\eta,t)}\right\}\\ \hat{\tau}_f(\eta,t) &= t - \frac{1}{2\pi}\partial_\eta \arg V_f(\eta,t) = t + \mathcal{R}e\left\{\frac{V_f^{tg}(\eta,t)}{V_f^g(\eta,t)}\right\},\end{aligned} \tag{13}$$

where $\hat{\omega}_f$ can be viewed as an approximation of the instantaneous frequency and $\hat{\tau}_f$ as the group delay. Then, the reassignment step aims to retrieve the ideal TF representation by moving the coefficients of the spectrogram according to the map $(\eta,t) \mapsto (\hat{\omega}_f(\eta,t), \hat{\tau}_f(\eta,t))$, which reads:

$$S_f(\omega,\tau) = \int_{\mathbb{R}}\int_0^\infty |V_f(\eta,t)|^2 \delta(\omega - \hat{\omega}_f(\eta,t))\delta(\tau - \hat{\tau}_f(\eta,t))\, d\eta dt. \tag{14}$$

B. STFT-Based SST

The aim of SST based on STFT (FSST), introduced in [1] in the CWT context, is to retrieve the ideal TF representation, i.e. TI_f with $s = 1$, from its STFT. Following [1], the authors in [17], [18] proposed to neglect operator $\hat{\tau}_f$, and to reassign only the complex coefficients $V_f(\eta,t)$ according to the map $(\eta,t) \mapsto (\hat{\omega}_f(\eta,t), t)$, which read:

$$T_f(\omega,t) = \frac{1}{g(0)}\int_0^\infty V_f(\eta,t)\delta\left(\omega - \hat{\omega}_f(\eta,t)\right)\, d\eta. \tag{15}$$

Knowing ϕ_k', the k^{th} mode can then be retrieved by considering:

$$f_k(t) \approx \int_{|\omega-\phi_k'(t)|<d} T_f(\omega,t) d\omega. \tag{16}$$

In a nutshell, SST reassigns the information in the TF plane and then makes use of this sharpened representation to recover the modes. The rationale behind equations (15) and (16) is the reconstruction formula

$$f(t) = \frac{1}{g(0)}\int_0^\infty V_f(\eta,t)\, d\eta, \tag{17}$$

but only considering a mode-related integration domain instead of $\mathbb{R}_+$. This enables us to retrieve the modes which was not possible with RM based on the spectrogram, but the representation is unfortunately less sharp as soon as the frequency modulation is not negligible. This difference between FSST and RM is further illustrated in section III-D.

C. Perfect Localization and Reconstruction

We now recall the main properties of FSST and RM in terms of TF localization and mode reconstruction. We first highlight for what type of signals they actually lead to the ideal TF representation and then consider a more general case.

1) Synchrosqueezing for Perturbations of Pure Waves: One can show that $\hat{\omega}_f$ actually matches the instantaneous frequency only for a pure tone $Ae^{2i\pi\omega t}$. In this case, FSST provides the ideal TF representation given by equation (12). More interesting is the study of the behavior of FSST on perturbations of pure waves as was done in [4] for SST based on CWT. The corresponding result is available in [18] and can be summarized as follows. Let us start by defining precisely the class of MCS we study.

Definition III.1. *Let $\varepsilon > 0$ and $\Delta \in (0,1)$. We define the set $\mathcal{B}_{\Delta,\varepsilon}$ of MCS where*

- *for all k, f_k satisfies: $A_k \in \mathcal{C}^1(\mathbb{R}) \bigcap L^\infty(\mathbb{R})$, $\phi_k \in \mathcal{C}^2(\mathbb{R})$, $\sup_t \phi_k'(t) < \infty$ and for all t, $A_k(t) > 0$, $\phi_k'(t) > 0$, $|A_k'(t)| \leq \varepsilon$ and $|\phi_k''(t)| \leq \varepsilon$.*
- *the f_k are separated with resolution Δ i.e. for all $k \in \{1, \cdots, K-1\}$ and for all t,*

$$\phi_{k+1}'(t) - \phi_k'(t) > 2\Delta.$$

We can then define the synchrosqueezing operator, using a function $\rho \in \mathcal{D}(\mathbb{R})$, the space of compactly supported smooth functions, such that $\int \rho = 1$, a threshold $\gamma > 0$ and an accuracy parameter $\delta > 0$:

$$T_f^{\delta,\gamma}(\omega,t) = \frac{1}{g(0)} \int_{|V_f(\eta,t)|>\gamma} V_f(\eta,t) \frac{1}{\delta} \rho\left(\frac{\omega - \hat{\omega}_f(\eta,t)}{\delta}\right) d\eta, \tag{18}$$

and finally state the main result.

Theorem III.1. *Let $f \in \mathcal{B}_{\Delta,\varepsilon}$ and $\nu \in (0, \frac{1}{2})$. Consider a window $g \in \mathcal{S}(\mathbb{R})$, the space of smooth functions with fast decaying derivatives, such that* $\operatorname{supp} \hat{g} \in [-\Delta, \Delta]$. *Then, if ε is small enough,*

- *$|V_f(\eta,t)| > \varepsilon^\nu$ only if there exists $k \in \{1 \cdots, K\}$ such that $(\eta,t) \in Z_k := \{(\eta,t) \,/\, |\eta - \phi_k'(t)| < \Delta\}$.*
- *For all $k \in \{1, \cdots, K\}$ and all pair $(\eta,t) \in Z_k$ such that $|V_f(\eta,t)| > \varepsilon^\nu$, one has*

$$|\hat{\omega}_f(\eta,t) - \phi_k'(t)| \leq \varepsilon^\nu. \tag{19}$$

- *For all $k \in \{1, \cdots, K\}$ there exists a constant C such that for all $t \in \mathbb{R}$,*

$$\left| \lim_{\delta \to 0} \left(\int_{|\omega - \phi_k'(t)| < \varepsilon^\nu} T_f^{\delta,\gamma}(\omega,t)\, d\omega \right) - f_k(t) \right| \leq C\varepsilon^\nu. \tag{20}$$

Equation (20) shows that the synchrosqueezing operator has to be summed up around the ridge, the

width of the interval being $2\varepsilon^\nu$. As in practice ε is not known, one chooses a parameter d instead. Mode f_k is hence estimated at time t from FSST T_f according to:

$$f_k(t) \approx \int_{\phi'_k(t)-d}^{\phi'_k(t)+d} T_f(\omega, t)\, d\omega. \tag{21}$$

Note that a similar approximation result was stated before in [17], but with stronger (global) assumptions on the mode separation f_k, instead of the local one in Def III.1.

2) Reassignment of Perturbations of Linear Chirps: It was shown in [11] that the reassignment operators perfectly localize linear chirps, i.e. modes with a linear instantaneous frequency and constant amplitude. More precisely, one can easily prove the following result.

Theorem III.2. *Consider a pure linear chirp $h(t) = Ae^{2i\pi\phi(t)}$, where ϕ is a polynomial of degree 2 and $A > 0$. Then, whenever the reassignment operators are defined one has $\hat{\omega}_h(\eta, t) = \phi'(\hat{\tau}_h(\eta, t))$.*

As the operators are local, this suggests that whenever the instantaneous frequency is quasi-linear and the amplitude slow-varying, the reassignment provides an accurate approximation of the ideal TF representation.

D. Illustrations

To illustrate the differences between FSST and RM, we use two synthetic test signals throughout this paper. One (signal 1) is made of low-order polynomial chirps, that behave locally as linear chirps, and the other one (signal 2) contains strongly nonlinear sinusoidal frequency modulations and singularities (points where $\phi'' = 0$). Figure 1 displays FSST and RM for these signals. Note that wherever the slope of the ridge $\phi''(t)$ is strong, RM gives a more concentrated representation than FSST.

To illustrate the specificity of FSST regarding invertibility, we display on Figure 2 the reconstruction process of each test signals from FSST. To compute an estimation of the ridges $(t, \phi'_k(t))$, knowing the number K of modes, we use the same algorithm as in [4] or [19], which computes a local minimum of the functional

$$E_f(\varphi) \;=\; \sum_{k=1}^{K} - \int_{\mathbb{R}} |T_f(t, \varphi_k(t))|^2 dt + \int_{\mathbb{R}} \left(\lambda \varphi'_k(t)^2 + \beta \varphi''_k(t)^2\right) dt, \tag{22}$$

where $(t, \varphi_k(t))$ is an estimator of the ridge $(t, \phi'_k(t))$, and λ and β are two positive parameters tuning the level of regularization. Other ridge detectors such as the one developed in [20] may of course be used instead but this is beyond the scope of the present paper.

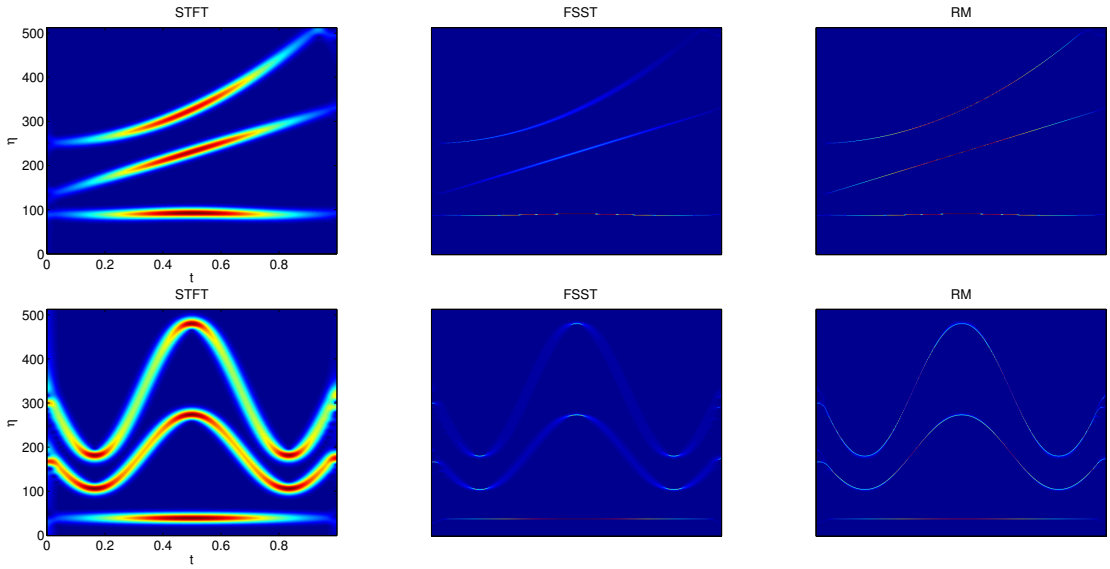

Figure 1. Illustration of FSST and RM for test signal 1 (top) and 2 (bottom). From left to right: the spectrogram, FSST and RM.

Looking at the results of Figure 2, it is worth noting that the quality of the reconstruction of a mode is highly dependent on its modulation. For instance mode 2 and 3 of signal 1 are properly retrieved but so is not mode 3 since it contains stronger modulations. Our goal is thus in what follows to improve mode reconstruction based on FSST when the modes are strongly modulated.

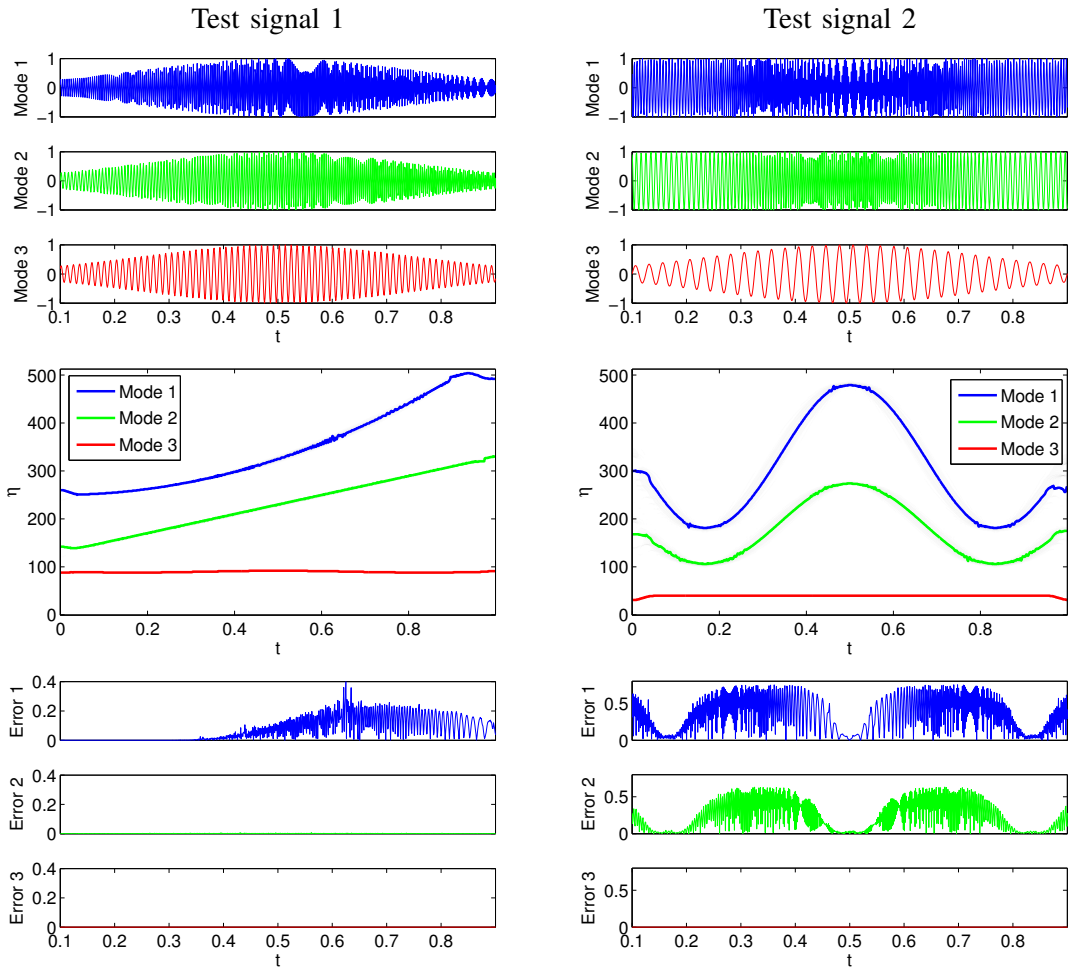

Figure 2. Illustration of mode retrieval based on SST on test signals 1 (left) and 2 (right). From top to bottom: the three modes making up the test signals, their SST with the estimated ridges superimposed, and the reconstruction error. SNR after reconstruction for modes 1, 2 and 3 equals 14, 51 and 70 dB for test signal 1, and 5, 7 and 70 dB for test signal 2, respectively. We use $d = 5$ in the reconstruction (see equation (21)).

IV. Towards a Second-Order FSST

Recalling that FSST was designed to process superpositions of perturbed pure waves, by second order FSST we mean that we want to adapt SST to superpositions of perturbed linear chirps. This should enable us to obtain an invertible sharpened TF representation of the same quality of the one provided by RM. To build our extension of SST, we are going to first consider the case of linear chirps, i.e. modes with constant amplitude and quadratic phase.

A. Handling Strong Modulations: Invertible Reassignment or Second-Order Synchrosqueezing?

Let us investigate here the case of linear chirps $h(t) = Ae^{2i\pi\phi(t)}$ with $\phi(t) = a + bt + \frac{1}{2}ct^2$. For such signals, one has for each t and τ:

$$h(\tau) = h(t)e^{i\pi c(\tau-t)^2}e^{2i\pi\phi'(t)(\tau-t)}, \tag{23}$$

which leads to:

$$V_h(\eta, t) = h(t)\int_{\mathbb{R}} g(\tau)e^{i\pi c\tau^2}e^{-2i\pi(\eta-\phi'(t))\tau}\,d\tau. \tag{24}$$

In such a case, the first reassignment operator writes

$$\hat{\omega}_h(\eta, t) = \phi'(t) - \frac{c}{2\pi}u(\eta - \phi'(t)), \tag{25}$$

where u is the function defined by:

$$u(\xi) = \frac{d}{d\xi}\arg\left\{\int_{\mathbb{R}} g(x)e^{i\pi cx^2}e^{-2i\pi\xi x}\,dx\right\}. \tag{26}$$

In the case of a Gaussian window g, one can show that u is linear [19], [21]. However, for a general smooth window g the exact nature of u is unknown, but one can remark that it is a smooth function. Formula (25) is directly derived from the first equation of (13). In the case of a linear chirp, one may write using (23, 24):

$$\begin{aligned}
\hat{\omega}_h(\eta, t) &= \frac{1}{2\pi}\partial_t \mathrm{arg} V_h(\eta, t) \\
&= \frac{1}{2\pi}\partial_t \mathrm{arg}\ h(t)\int_{\mathbb{R}} g(\tau)e^{i\pi c\tau^2}e^{-2i\pi(\eta-\phi'(t))\tau}\,d\tau \\
&= \frac{1}{2\pi}\partial_t\left[2\pi\phi(t) + \arg\ \int_{\mathbb{R}} g(\tau)e^{i\pi c\tau^2}e^{-2i\pi(\eta-\phi'(t))\tau}\,d\tau\right] \\
&= \phi'(t) + \frac{1}{2\pi}\partial_t(\eta - \phi'(t))\ u(\eta - \phi'(t)) \\
&= \phi'(t) - \frac{c}{2\pi}u(\eta - \phi'(t)).
\end{aligned}$$

Equation (25) clearly shows that $\omega_h(\eta, t) = \phi'(t)$ does not hold as soon as $c \neq 0$. We propose two different ways to deal with the non-negligible modulation $c = \phi''(t)$. The first one consists in modifying the first reassignment operator by taking into account second-order terms, and then use this operator to define a new SST. Since reassignment will only take place in the direction of the frequencies, we will call it VSST (V for vertical) in the sequel.

The second one uses the local time delay $\hat{\tau}_h$ defined in RM, which writes for linear chirps:

$$\hat{\tau}_h(\eta,t) = t - \frac{1}{2\pi}u(\eta - \phi'(t)), \tag{27}$$

which is derived from the second equation of (13):

$$\begin{aligned}\hat{\tau}_f(\eta,t) &= t - \frac{1}{2\pi}\partial_\eta \arg V_f(\eta,t)\\ &= t - \frac{1}{2\pi}\partial_\eta \text{arg}\int_{\mathbb{R}} g(\tau)e^{i\pi c\tau^2}e^{-2i\pi(\eta-\phi'(t))\tau}\,d\tau\\ &= t - \frac{1}{2\pi}u(\eta-\phi'(t))\end{aligned}$$

Remembering that $\phi'(t) = b + ct$, we get from (25) and (27) that:

$$\hat{\omega}_h(\eta,t) = \phi'(\hat{\tau}_h(\eta,t)), \tag{28}$$

which means $\hat{\omega}_h(\eta,t)$ is the exact value of ϕ' but at a shifted time location given by $\hat{\tau}(\eta,t)$. This is not surprising since RM is well known to perfectly localize linear chirps. The challenge here lies in designing a complex reassignment formula which allows for mode reconstruction. Since the proposed technique will use the two components of the reassignment vector we will call it OSST (O for oblique).

B. Local Instantaneous Modulation

Both VSST and OSST will use an estimation of the frequency modulation, $\hat{q}_f$, whose definition follows:

Definition IV.1. *Let f be in $L^2(\mathbb{R})$. $\hat{q}_f(\eta,t)$ is defined wherever $V_f(\eta,t) \neq 0$ and $\partial_t\hat{\tau}_f(\eta,t) \neq 0$ by:*

$$\hat{q}_f(\eta,t) = \frac{\partial_t\hat{\omega}_f(\eta,t)}{\partial_t\hat{\tau}_f(\eta,t)}. \tag{29}$$

The following result shows that the local operator $\hat{q}_f(\eta,t)$ perfectly estimates the frequency modulation $c = \phi''(t)$ for a linear chirp.

Proposition IV.1. *If $h(t) = Ae^{2i\pi\phi(t)}$ is a linear chirp, ie $\phi''(t) = \phi'' \neq 0$, then for each (η,t) where $\hat{q}_h$ is defined, one has*

$$\hat{q}_h(\eta,t) = \phi''. \tag{30}$$

Otherwise $\hat{q}_h(\eta,t)$ can be computed through the general formula:

$$\hat{q}_h(\eta,t) = \mathcal{I}m\left\{\frac{1}{2\pi}\frac{(V_h^{g'})^2 - V_h^{g''}V_h^g}{V_h^{xg}V_h^{g'} - V_h^{xg'}V_h^g}\right\}, \tag{31}$$

where $V_h^{g''}$ and $V_h^{xg'}$ are the STFT of h with windows g'' and $x \mapsto xg'(x)$.

Proof. Let us first recall that for a linear chirp equation (28) holds, i.e $\hat{\omega}_h(\eta,t) = \phi'(\hat{\tau}_h(\eta,t))$. Then differentiating this equality with respect to t, one obtains: $\partial_t\hat{\omega}_h(\eta,t) = \phi''(\hat{\tau}_h(\eta,t))\partial_t\hat{\tau}_h(\eta,t)$ or equivalently $\hat{q}_h(\eta,t) = \phi''(\hat{\tau}_h(\eta,t))$. Now since ϕ'' is constant, this leads to the expected result.

Regarding the computation of $\hat{q}_h$, recall that for any signal f,

$$\partial_t V_f^g(\eta,t) = -V_f^{g'}(\eta,t) + 2i\pi\eta V_f^g(\eta,t).$$

To lighten the notation, we will note V_h^g for $V_h^g(\eta,t)$. Equation (13) gives

$$\begin{aligned}
\partial_t\hat{\omega}_h &= \partial_t\left(\eta + \mathcal{I}m\left\{\frac{1}{2\pi}\frac{V_h^{g'}}{V_h^g}\right\}\right)\\
&= \mathcal{I}m\left\{\frac{1}{2\pi}\frac{\partial_t V_h^{g'}V_h^g - V_h^{g'}\partial_t V_h^g}{(V_h^g)^2}\right\}\\
&= \mathcal{I}m\left\{\frac{1}{2\pi}\frac{(-V_h^{g''} + 2i\pi\eta V_h^{g'})V_h^g - V_h^{g'}(-V_h^{g'} + 2i\pi\eta V_h^g)}{(V_h^g)^2}\right\}\\
&= \mathcal{I}m\left\{\frac{1}{2\pi}\frac{(V_h^{g'})^2 - V_h^{g''}V_h^g}{(V_h^g)^2}\right\}.
\end{aligned}$$

Similarly one has

$$\begin{aligned}
\partial_t\hat{\tau}_h &= \partial_t\left(t + \mathcal{R}e\left\{\frac{V_h^{xg}}{V_h^g}\right\}\right)\\
&= 1 + \mathcal{R}e\left\{\frac{\partial_t V_h^{xg}V_h^g - V_h^{xg}\partial_t V_h^g}{(V_h^g)^2}\right\}\\
&= 1 + \mathcal{R}e\left\{\frac{(-V_h^g - V_h^{xg'} + 2i\pi\eta V_h^{xg})V_h^g - V_h^{xg}(-V_h^{g'} + 2i\pi\eta V_h^g)}{(V_h^g)^2}\right\}\\
&= \mathcal{R}e\left\{\frac{V_h^{xg}V_h^{g'} - V_h^{xg'}V_h^g}{(V_h^g)^2}\right\}.
\end{aligned}$$

□

C. Vertical Second-Order Synchrosqueezing

Let $h(t) = Ae^{2i\pi\phi(t)}$ be a linear chirp with constant FM ϕ''. Equations (25) and (27) show that for any time t,

$$\begin{aligned} \phi'(t) &= \phi'(\hat{\tau}_h(\eta,t)) + \phi''(\hat{\tau}_h(\eta,t))(t - \hat{\tau}_h(\eta,t)) \\ &= \hat{\omega}_h(\eta,t) + \hat{q}_h(\eta,t)(t - \hat{\tau}_h(\eta,t)), \end{aligned} \tag{32}$$

which means that the first order Taylor expansion of ϕ' can be written in terms of the first reassignment and frequency modulation operators. Using locally the chirp approximation for a given signal f, one can now improve the estimation of the instantaneous frequency as follows:

Definition IV.2. *Let $f \in L^2(\mathbb{R})$, we define the second-order instantaneous frequency estimator of f by:*

$$\tilde{\omega}_f(\eta,t) = \begin{cases} \hat{\omega}_f(\eta,t) + \hat{q}_f(\eta,t)(t - \hat{\tau}_f(\eta,t)) & \text{if } \partial_t \hat{\tau}_f(\eta,t) \neq 0 \\ \hat{\omega}_f(\eta,t) & \text{otherwise.} \end{cases}$$

The vertical second-order synchrosqueezing (VSST) then consists in replacing $\hat{\omega}$ by $\tilde{\omega}$ in standard SST:

$$TV_f(\eta,t) = \frac{1}{g(0)} \int_{\mathbb{R}} V_f(\eta,t)\delta\left(\omega - \tilde{\omega}_f(\eta,t)\right) d\eta \tag{33}$$

Since the coefficients are only moved vertically, the reconstruction is still achievable by summing up the SST coefficients in the vicinity of the ridge. Moreover, as all the operators are local, VSST should remain efficient for small perturbations of linear chirps. This will be further studied numerically in the next section.

D. Oblique Synchrosqueezing

An alternative way to modify FSST to take into account FM consists in moving the coefficients according to the reassignment vector field while keeping the phase information so as to allow signal reconstruction. A first attempt in this direction defined the following complex reassigned transformation [14]:

$$TC_f(\omega,\tau) = \iint_{\mathbb{R}^2} V_f(\eta,t) e^{i\pi(\omega+\eta)(\tau-t)} \delta\left(\omega - \hat{\omega}_f(\eta,t)\right) \delta\left(\tau - \hat{\tau}_f(\eta,t)\right) d\eta dt. \tag{34}$$

Unfortunately, this definition allowed for an approximative reconstruction only for Gaussian windows, and with non-negligible errors as demonstrated by numerical results.

Let us now propose an alternative reassignment technique computing the phase shift in a different way

from [14] and that we will call oblique synchrosqueezing (OSST). The starting point is to remark that the STFT of a linear chirp h is invariant by translations along the direction of the ridge $(ct,t)\,, t \in \mathbb{R}$ modulo a phase shift. Indeed, one can write, using (24) and $\phi'(t) = b + ct$,

$$\begin{aligned} V_h(\eta,t) &= h(t)\int_{\mathbb{R}} g(s)e^{i\pi cs^2}e^{-2i\pi s(\eta-\phi'(t))}\,ds \\ &= e^{2i\pi\phi(t)}\int_{\mathbb{R}} g(s)e^{i\pi cs^2}e^{-2i\pi s(\eta+c(\tau-t)-\phi'(\tau))}\,ds \\ &= V_h(\eta+(\tau-t)c,\tau)e^{2i\pi(\phi(t)-\phi(\tau))} \\ &= V_h(\eta+(\tau-t)c,\tau)e^{2i\pi(t-\tau)(\phi'(\tau)+\frac{c}{2}(t-\tau))}. \end{aligned} \tag{35}$$

Instead of reassigning the real value $|V_h(\eta,t)|^2$ as in RM, we propose to move the complex quantity

$$V_h(\eta,t)e^{2i\pi(\tau-t)(\phi'(\tau)-\frac{c}{2}(\tau-t))} = V_h(\eta+(\tau-t)c,\tau)$$

Contrary to VSST where one builds a first order Taylor expansion of the derivative of the phase, OSST directly involve the phase shift. For a linear chirp and when $\tau = \hat{\tau}_h(\eta,t)$, one has $\phi'(\tau) = \hat{\omega}_h(\eta,t)$ so that one can then write:

$$V_h(\eta,t)e^{2i\pi(\tau-t)(\hat{\omega}_h(\eta,t)-\frac{\hat{q}_h(\eta,t)}{2}(\tau-t))} = V_h(\eta+(\tau-t)c,\tau).$$

This phase-modified coefficients belong to the vertical line $I'_\tau = \{(\eta,\tau)\,/\,\eta \in \mathbb{R}\}$. Finally, summing up all the phase shifted coefficients along the frequency axis will provide an approximation of h at time τ.

The principle of OSST is illustrated on Figure 3: the coefficients making up the dashed curve are phase-shifted while moved to point (ω,τ). To obtain an approximation of the signal $h(\tau)$, the phase of the coefficients are modified in order to be equal to their projection on the dashed dotted line.

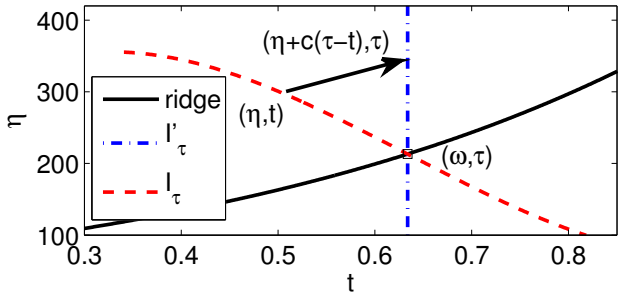

Figure 3. Illustration of oblique synchrosqueezing (OSST).

Let us now give a more formal definition of OSST.

Definition IV.3. *Let $f \in L^2(\mathbb{R})$, its oblique synchrosqueezing (OSST) is the function*

$$TO_f(\omega,\tau) = \frac{1}{g(0)} \iint_{\mathbb{R}^2} V_f(\eta,t) e^{i\pi(2\omega - \hat{q}_f(\eta,t)(\tau-t))(\tau-t)} \delta\left(\omega - \hat{\omega}_f(\eta,t)\right) \delta\left(\tau - \hat{\tau}_f(\eta,t)\right) \, d\eta dt. \quad (36)$$

An approximation of mode f_k is then given by its OSST on the ridge, i.e.

$$f_k(t) \approx TO_f(\phi_k'(t), t). \quad (37)$$

As for FSST and VSST, we would like OSST to remain efficient for perturbations of linear chirps, when the amplitude (resp. phase) is not exactly constant (resp. quadratic). Recall that for SST, the strategy to handle such perturbations was to integrate the coefficients around the ridge, so as to compensate for the error made by estimating the instantaneous frequency by $\hat{\omega}_f$. However, in the case of OSST the coefficients are moved both in time and frequency, making this regularization impossible. We will see in the next section how this impacts the performance of the proposed technique.

V. Numerical results

To achieve a quantitative comparison between the different methods, we will reuse the test signals defined in section III-D. Recall that test signal 1 is made of quasi-linear chirps that should be well dealt with by VSST or OSST, while test signal 2 contains stronger nonlinear frequency modulations as well as singularities where $\phi''(t)$ vanishes, which makes the study of such signals more difficult. For the sake of simplicity, we only consider the case of FSST, but similar results could be obtained within the wavelet framework (see for instance [18] for a comparison). Note that in our simulations, we use a Gaussian window with parameter $\sigma = 0.05$, defined by $g(t) = \sigma^{-\frac{1}{2}} e^{-\frac{\pi t^2}{\sigma^2}}$.

On Figure 4 SST, VSST and OSST of both signals 1 and 2 are depicted. Comparing with Figure 1, one notices that both VSST and OSST provide a nice TF representation, as sharp as RM. In the next subsections, we will compare more quantitatively the three methods in terms of the sparseness of the representation (i.e. the number of nonzero coefficients) and accuracy of mode reconstruction. We also numerically investigate the robustness to noise, and finally compare the methods on some real data.

A. Quality of Representation

The main purpose of RM was to make TF representations more readable, more easily interpretable. Since readability is somewhat subjective, we propose here to measure the readability as the amount

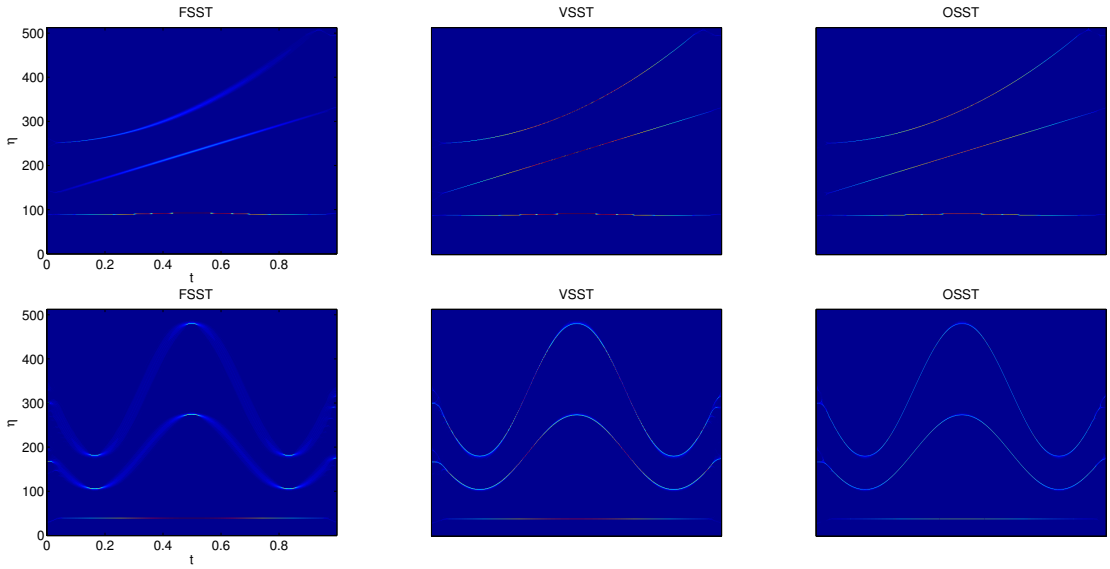

Figure 4. Test signals number 1 (top) and 2 (bottom). From left to right, magnitude of FSST, OSST and VSST.

of information contained in the nonzero coefficients of the decomposition. In this regard, one way to compare the different representations is to compute the normalized energy associated with the N first coefficients with the largest amplitude: the faster the growth of this energy towards 1, the sharper the representation. Figure 5 displays this normalized energy (i.e., the cumulative sum of the first N squared sorted coefficients) for both test signals and the five representations, namely STFT, RM, FSST, VSST and OSST. The first remark is that both OSST and VSST behave similarly as RM for both test signals. Indeed, the representation of test-signal 1 with each of these three methods is almost perfect, since one needs only 3 coefficients per time instant to recover the signal energy, which is consistent with the three modes making up the test signal. Comparatively, the energy of FSST grows rapidly to reach a value around 80% and then stagnates which means the signal energy cannot be retrieved with a reasonnable number of coefficients. The results are similar but less sharp for the second test-signal, since it contains stronger nonlinear frequency modulations.

In order to visualize the influence of noise, we carry out the same experiments when the test signals are contaminated by white Gaussian noise. We use a strong noise level (0 dB) and display the results on Figure 6. We observe that the increase of the energy is slower, since the coefficients corresponding to noise are spread out in the whole TF plane. However, OSST, RM and VSST still behave better than FSST, even though VSST is slightly less competitive.

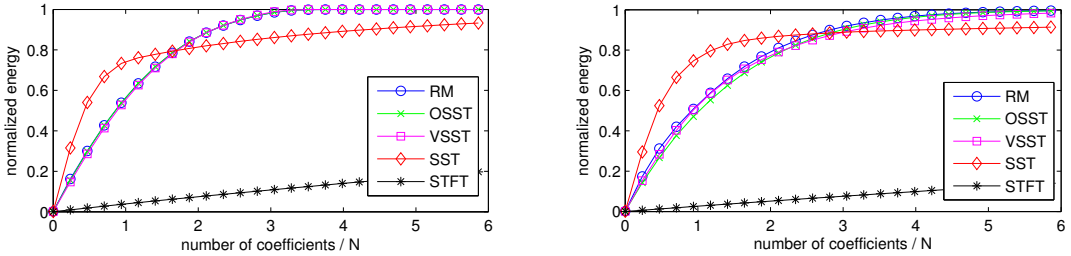

Figure 5. Normalized energy as a function of the number of coefficients for test-signal 1 (left) and 2 (right). Abscissa gives the number of coefficients over the size N of the signal, i.e. the mean number of coefficients for each column of the TF plane.

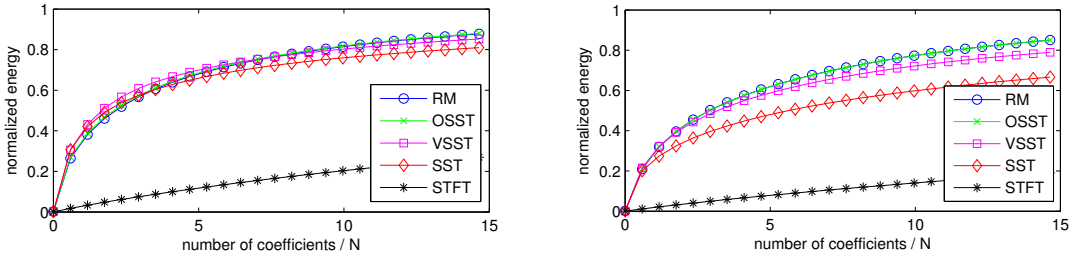

Figure 6. Normalized energy as a function of the number of coefficients for the noisy (0 dB) test-signal 1 (left) and 2 (right).

B. Reconstruction of the Modes

The main advantage of FSST over RM is its invertibility. Let us recall that there are two possible reconstructions of the mode from FSST. The easiest one assumes T_f is almost ideal, so that the whole information is concentrated on the ridge. The mode f_k at time t is then estimated following

$$f_k(t) \approx T_f(\phi'_k(t), t). \tag{38}$$

FSST allows to achieve a more accurate reconstruction by using an integration around the ridge as a regularization step, according to the formula

$$f_k(t) \approx \int_{-d}^{d} T_f(\phi'_k(t) + \xi, t)\, d\xi. \tag{39}$$

Provided d is of the same order of magnitude as the perturbation defined in Theorem III.1, the latter ensures an asymptotically perfect reconstruction. We investigate here the accuracy of the reconstruction for each method starting with the reconstruction technique defined in (38). The results measuring the accuracy of mode reconstruction displayed in terms of SNR are displayed in Table I. We check that both OSST and VSST enable a good reconstruction of polynomial chirps (signal-test 1), whereas the quality

	SST	OSST	VSST	Gardner
Test signal 1	3.5	17	**18**	11
Mode 1	1.5	15	**16**	8.8
Mode 2	2.2	17	**19**	12
Mode 3	**19**	**19**	**19**	**19**
Test signal 2	2.2	**8.9**	7.6	5.6
Mode 1	0.92	**7.4**	5.9	3.8
Mode 2	1.4	**8.4**	7.2	5.3
Mode 3	**57**	23	**57**	23

Table I
Direct reconstruction for each method, and both test signals. The accuracy of mode retrieval is expressed in SNR.

of direct reconstruction from FSST is very poor. Looking at the results for each mode, one observes that all the methods achieve a good reconstruction for mode 3 since it is not modulated, whereas FSST is unadapted for modes 1 and 2 which contain stronger modulations. The results are less convincing for test-signal 2: even if OSST and VSST improve the reconstruction compared to FSST, the accuracy is far from satisfactory. Indeed, as this signal contains strongly nonlinear frequency modulations, both OSST and VSST fail to represent the modes as a perfect sharp curve in the TF plane, some information being spread out around the ridges. This result is in line with the simulation of Figure 6 right, where on average 4 coefficients per time instant are needed to recover the most part of the energy.

In order to compensate for that default, one has to integrate the transformations when possible around the ridge, following equation (39). The results for such a reconstruction are displayed on Figure 7. For each test signal, the SNR of the reconstruction is displayed with respect to parameter d. This time we display the SNR associated with the reconstruction of the whole signal but considering the modes individually would lead to the same results. Figure 7 shows that VSST allows for a quasi-perfect reconstruction from very few coefficients ($\mathrm{SNR} = 50\,\mathrm{dB}$ for $d \geq 3$). Conversely, with FSST, even if one uses a large d, i.e. many coefficients, one cannot retrieve the modes with a high accuracy.

We already saw that in the noise-free case, the reconstruction is all the better that parameter d is large. This is obviously not true when the signal is contaminated by noise: d must be large enough to take into account the signal coefficients, while remaining small enough so as not to include too much noise in the reconstruction. We illustrate this quantitatively by making the same experiments as for Figure 7 but in the noisy case. Note that in this case, the estimation of the ridges using formula (22) is worsened due to the presence of noise. The results of the ridge estimation are depicted on Figure 8, together with the reconstruction accuracy, for both FSST and VSST and with a moderate noise level ($\mathrm{SNR} = 12\,\mathrm{dB}$).

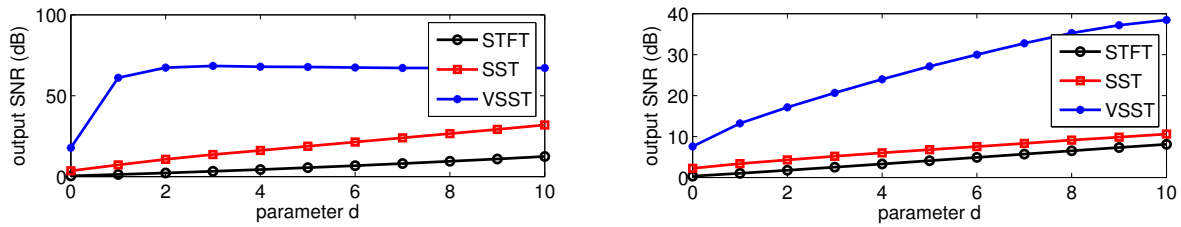

Figure 7. Reconstruction of the modes as a function of d, which is proportional to the size of the interval of integration. The results are in SNR, for test signal 1 (left) and 2 (right).

While the ridge estimation can be successfully carried out on FSST and VSST for test-signal 1, only VSST gives a correct estimation for test-signal 2 since the latter contains stronger FMs. As a result, the reconstruction of test-signal 2 from SST cannot be satisfactory. This study tells us that to take into account second order terms in the definition of VSST not only improves the quality of mode reconstruction but also of ridge detection.

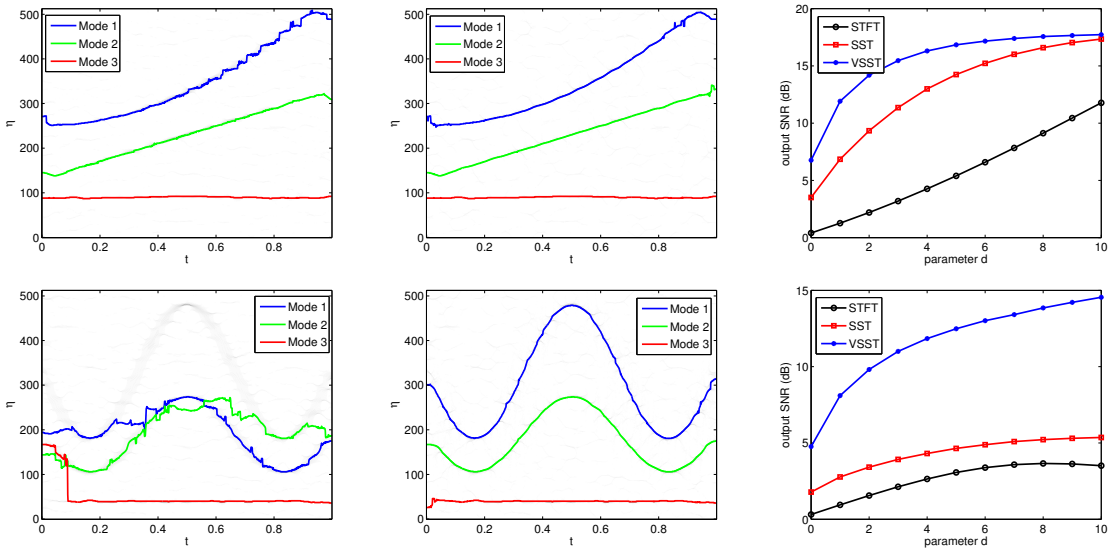

Figure 8. From left to right: the ridges estimated from FSST, those estimated from VSST, and the quality of reconstruction measured as a function of d. We use again test signal 1 (top) and 2 (bottom).

C. Illustration on Real Signals

We now illustrate the qualitative improvement of the two new transformations on real data. We start by considering a bat echolocation call, available at http://dsp.rice.edu/sites/dsp.rice.edu/files/software/batsignal.zip. Figure 9 displays both VSST and OSST of this signal, and compare them with the

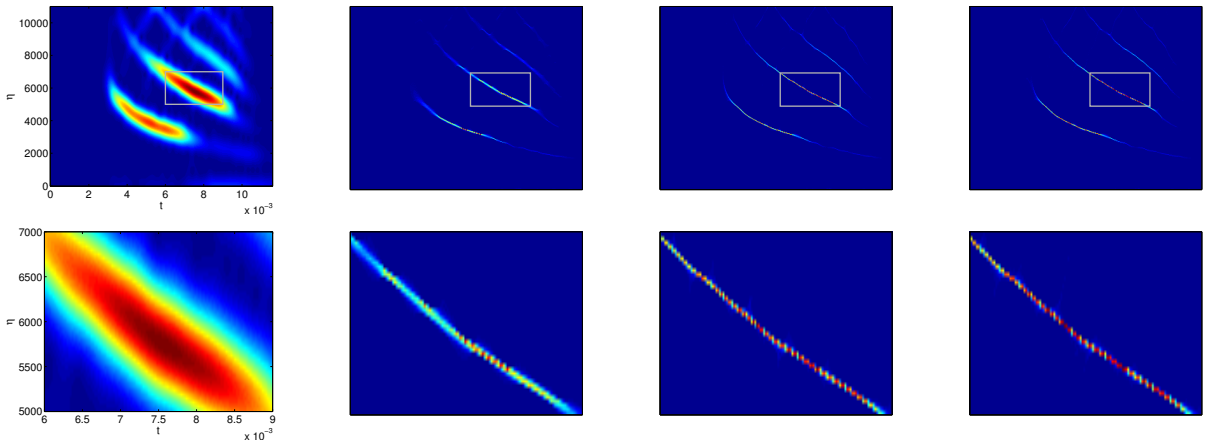

Figure 9. TF representations of a bat echolocation call. The representations are (from left to right) STFT, FSST, OSST and VSST. A zoom on strong modulations is displayed in the second row.

spectrogram and FSST (parameter σ being set to 0.04). By zooming around a portion of one ridge, the improvement brought about these new methods in terms of concentration and compactness of the representation is undeniable. Note that the result provided by FSST remains satisfactory since the frequency modulation is quite slow compared to the size of the window.

To better illustrate that improvement, we then considered a portion of a speech signal, with parameter σ set to 0.025. Figure 10 shows the corresponding TF representations associated with the four different methods, as well as a zoom on a modulated portion. For both VSST and OSST, the energy of the representation is almost perfectly concentrated along the ridges whereas FSST does not provide an as sharp representation. Note that the representation given by OSST seems slightly better but we know by now that VSST provides with a more reliable reconstruction technique.

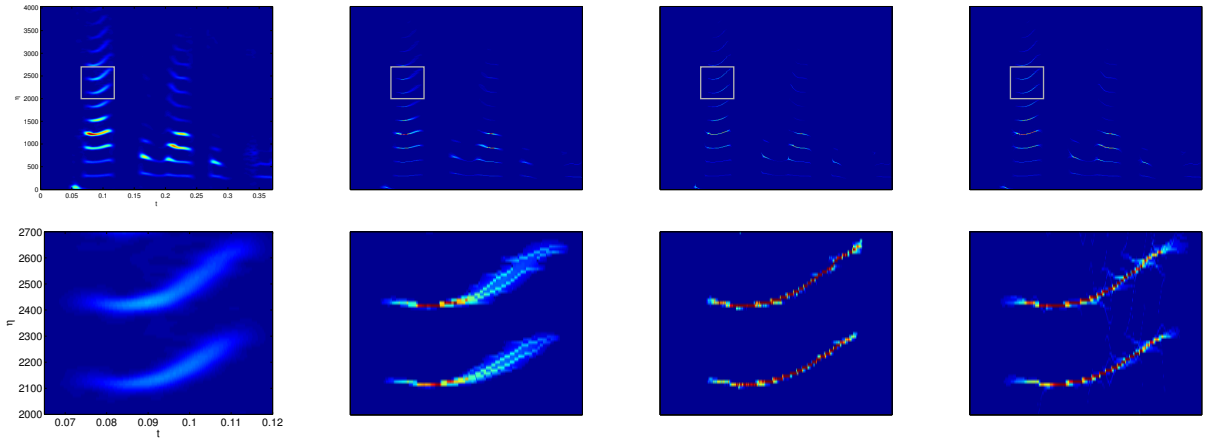

Figure 10. TF representations of a speech signal. The representations are (from left to right) STFT, FSST, OSST and VSST. A zoom on a strongly modulated part is displayed on the second row.

VI. Conclusion

This paper introduced the vertical and oblique second-order synchrosqueezing transformations to circumvent the limitations of standard SST and reassignment. We emphasized that OSST can be viewed as a complex version of the reassignment method, whereas VSST keeps the fixed-time structure of the standard synchrosqueezing transform, allowing for a better reconstruction through a regularization step. We showed that both methods provide the ideal invertible representation in the case of a linear chirp, while remaining efficient on general multicomponent signals containing strong frequency modulations. All the experiments suggest that OSST is slightly more competitive for the representation purpose, whereas VSST allows for a better reconstruction.

Note that both the OSST and VSST can be extended readily to the wavelet setting. Further work should be devoted to the theoretical analysis of both methods for perturbations of linear chirps, as well as a precise understanding of the influence of noise on the reassignment operators and on the ridge estimation.

References

[1] I. Daubechies and S. Maes, "A nonlinear squeezing of the continuous wavelet transform based on auditory nerve models," *Wavelets in Medicine and Biology*, pp. 527–546, 1996.

[2] N. E. Huang, Z. Shen, S. R. Long, M. C. Wu, H. H. Shih, Q. Zheng, N.-C. Yen, C. C. Tung, and H. H. Liu, "The empirical mode decomposition and the Hilbert spectrum for nonlinear and non-stationary time series analysis," *Proceedings of the Royal Society of London. Series A: Mathematical, Physical and Engineering Sciences*, vol. 454, no. 1971, pp. 903–995, 1998.

[3] G. Rilling, P. Flandrin, P. Goncalves *et al.*, "On empirical mode decomposition and its algorithms," in *IEEE-EURASIP Workshop on Nonlinear Signal and Image Processing NSIP*, vol. 3, 2003, pp. 8–11.

[4] I. Daubechies, J. Lu, and H.-T. Wu, "Synchrosqueezed wavelet transforms: an empirical mode decomposition-like tool," *Applied and computational harmonic analysis*, vol. 30, no. 2, pp. 243–261, 2011.

[5] M. Skolnik, *Radar handbook*. McGraw-Hill, 1970.

[6] J. W. Pitton, L. E. Atlas, and P. J. Loughlin, "Applications of positive time-frequency distributions to speech processing," *Speech and Audio Processing, IEEE Transactions on*, vol. 2, no. 4, pp. 554–566, 1994.

[7] E. J. Candes, P. R. Charlton, and H. Helgason, "Detecting highly oscillatory signals by chirplet path pursuit," *Applied and Computational Harmonic Analysis*, vol. 24, no. 1, pp. 14–40, 2008.

[8] L. Cohen, *Time-frequency analysis: theory and applications*. Prentice-Hall, Inc., 1995.

[9] P. Flandrin, *Time-frequency/time-scale analysis*. Academic Press, 1998, vol. 10.

[10] K. Kodera, C. De Villedary, and R. Gendrin, "A new method for the numerical analysis of non-stationary signals," *Physics of the Earth and Planetary Interiors*, vol. 12, no. 2, pp. 142–150, 1976.

[11] F. Auger and P. Flandrin, "Improving the readability of time-frequency and time-scale representations by the reassignment method," vol. 43, no. 5, pp. 1068–1089, 1995.

[12] C. Li and M. Liang, "A generalized synchrosqueezing transform for enhancing signal time–frequency representation," *Signal Processing*, vol. 92, no. 9, pp. 2264–2274, 2012.

[13] S. Wang, X. Chen, G. Cai, B. Chen, X. Li, and Z. He, "Matching demodulation transform and synchrosqueezing in time-frequency analysis," 2013.

[14] T. Gardner and M. Magnasco, "Sparse time-frequency representations," *Proceedings of the National Academy of Sciences*, vol. 103, no. 16, pp. 6094–6099, 2006.

[15] A. Grossmann and J. Morlet, "Decomposition of Hardy functions into square integrable wavelets of constant shape," *SIAM journal on mathematical analysis*, vol. 15, no. 4, pp. 723–736, 1984.

[16] I. Daubechies, "The wavelet transform, time-frequency localization and signal analysis," *Information Theory, IEEE Transactions on*, vol. 36, no. 5, pp. 961–1005, 1990.

[17] H.-T. Wu, "Adaptive analysis of complex data sets," *PhD, Princeton University*, 2012.

[18] T. Oberlin, S. Meignen, and V. Perrier, "The Fourier-based synchrosqueezing transform," in *39th International Conference on Acoustics, Speech, and Signal Processing, ICASSP 2014*, 2014.

[19] F. Auger, P. Flandrin, Y. Lin, S. McLaughlin, S. Meignen, T. Oberlin, and H. Wu, "Time-frequency reassignment and synchrosqueezing: An overview," *Signal Processing Magazine, IEEE*, vol. 30, no. 6, pp. 32–41, 2013.

[20] R. Carmona, W. Hwang, and B. Torrésani, "Multiridge detection and time-frequency reconstruction," vol. 47, no. 2, pp. 480–492, 1999.

[21] T. Oberlin, S. Meignen, and S. Mclaughlin, "Analysis of strongly modulated multicomponent signals with the short-time Fourier transform," in *38th International Conference on Acoustics, Speech, and Signal Processing, ICASSP 2013*, 2013.